Translational Oncology 49 (2024) 102106

Contents lists available at ScienceDirect

Translational Oncology

journal homepage: www.elsevier.com/locate/tranon

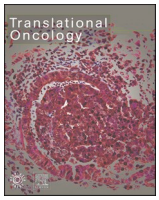

Original Research

Low cytoplasmic NUB1 protein exerts hypoxic cell death with poorer prognosis in oestrogen receptor negative breast cancer patients

Ka-Liong Tan [a,e,*], Syed Haider [b,c,f], Christos E. Zois [b], Jianting Hu [a], Helen Turley [b], Russell Leek [b], Francesca Buffa [c], Oreste Acuto [d], Adrian L. Harris [b], Francesco Pezzella [a,**]

[a] Tumour Pathology Laboratory, Nuffield Division of Clinical Laboratory Sciences, Radcliffe Department of Medicine, John Radcliffe Hospital, Headington, Oxford OX3 9DU, UK
[b] Department of Oncology, University of Oxford, Old Road Campus Research Building, Roosevelt Drive, Oxford, OX3 7DQ, UK
[c] Computational Biology and Integrative Genomics, Department of Oncology, Old Road Campus Research Building, Roosevelt Drive Oxford, University of Oxford, UK
[d] Laboratory of T-cell signalling, Sir William Dunn School of Pathology, University of Oxford, Oxford OX1 3RE, UK
[e] Faculty of Medicine and Health Sciences, Universiti Sains Islam Malaysia (USIM), Persiaran Ilmu, Putra Nilai, 71800 Nilai, Negeri Sembilan, Malaysia
[f] The Breast Cancer Now Toby Robins Breast Cancer Research Centre, The Institute of Cancer Research, London, SW3 6JB, UK

ARTICLE INFO

Keywords:
NUB1
Oestrogen receptor
Immunohistochemistry
Biomarkers

ABSTRACT

Current prognostic biomarkers fall short in stratifying Oestrogen receptor (ER)-negative breast cancer patients regarding tumour progression risk at diagnosis. The role of AIPL1 in activating its tumour suppressor client protein, NEDD8 Ultimate Buster-1 (NUB1) remains unknown in cancer. Our study demonstrated how down-regulated AIPL1 results in the deactivated NUB1 protein under hypoxic conditions. We examined the AIPL1-NUB1 pathway*in vitro* using cell lines i.e. MCF-7, MDA-MB-231, RCC4 *etc.* NUB1 expression was assessed using Oncomine, and cBioPortal was performed to assess NUB1′s prognostic significance in human cancers. In the John Radcliffe Hospital cohort ($n = 122$), immunohistochemistry analysis revealed downregulated AIPL1 (Log2 fold change=-0.28; $p < 0.001$) and upregulated NUB1 transcripts (Log2 fold change=0.59; $p < 0.001$) compared to adjacent normal tissues. In severe chronic hypoxia, multimerised AIPL1 localisedin the cytoplasm while NUB1 protein migrated to the nucleus, where the absence of NUB1 nuclear localisation led to cell cycle arrest. Biopsies showed that patients with lower cytoplasmic NUB1 expression ($n = 57$) had poorer overall survival compared to those with higher cytoplasmic expression ($n = 57$), HR=1.78; 95 % CI=1.01–3.35, $p = 0.048$. Low NUB1 protein levels in both normoxic and hypoxic conditions were associated with cell cycle arrest and upregulation ofp21 and p27 in breast cancer cell lines, correlating significantly withpoorer survival outcomes in all breast cancer and ER-negative breast cancer patients.

Introduction

Heat shock proteins (HSPs) are elevated in a range of cancers, offering important diagnostic, prognostic, and treatment implications. They play a crucial role in the cancer proteome by assisting with protein assembly, secretion, trafficking, degradation, and the regulation of transcription factors. HSPs help maintain the conformation and function of client proteins, which affects tumour cell proliferation, differentiation, invasion, death, and immune system recognition [1]. Analysis of two mRNA microarray studies found that HSP genes, including Parkinsonism Associated Deglycase (PARK7), TNF Receptor Associated Protein 1 (TRAP1), VHL Binding Protein 1 (VBP1), and Aryl Hydrocarbon Receptor-Interacting Protein-Like 1 (AIPL1), were significantly down-regulated in tumours [2]. Reduced levels of HSPs in tumours might offer a growth advantage [3], as downregulated HSPs can affect tumour suppressor genes like TRAP1 in retinoblastoma [4] and VBP1 in Von Hippel-Lindau [5]. This led us to hypothesisethat tumour growth mechanisms involve the absence of HSPs, resulting in the inactivation of tumour suppressor proteins [2,3].

A meta-analysis of 30 microarray datasets confirmed reduced

* Corresponding author at: Faculty of Medicine & Health Sciences, University Sains Islam Malaysia, Persiaran Ilmu, Putra Nilai, 71800 Nilai, Negeri Sembilan, Malaysia.
** Corresponding author at: Tumour Pathology Laboratory, Nuffield Division of Clinical Laboratory Sciences, Radcliffe Department of Medicine, John Radcliffe Hospital, Headington, Oxford OX3 9DU, UK.
E-mail addresses: kaliong_tan@usim.edu.my (K.-L. Tan), Syed.Haider@icr.ac.uk (S. Haider), francesco.pezzella@ndcls.ox.ac.uk (F. Pezzella).

https://doi.org/10.1016/j.tranon.2024.102106
Received 23 April 2024; Received in revised form 27 July 2024; Accepted 18 August 2024
Available online 24 August 2024

expression of the HSP AIPL1 in cancer [2]. In datasets includingB cell lymphomas, bladder, renal, and colon cancers, AIPL1 transcription was notably down-regulated [6-9]. AIPL1 protein interacts with NEDD8 Ultimate Buster-1 (NUB1) in a chaperone-like manner [10], suppressing NUB1aggregation and facilitating its nuclear translocation [10]. NUB1, an interferon (IFN)-inducible protein composed of 601 amino acids, has a splice variant, NUB1L, withan extra 14 amino acids to encode an additional Ub-associated (UBA) domain. NUB1 proteins recruit FAT10- and NEDD8-conjugated proteins to the proteasome for degradation [11-14]. Therefore, the loss of AIPL1 protein deactivates NUB1 in vivo, impairing its nuclear translocation [10].

First described in 2000 [15], AIPL1's function remains unclear. It has only been reported in the pineal gland, retinal cells [16] and neurons [17]. The only known AIPL1 client protein, NUB1, is considereda potential tumour suppressor [12,18]. Genetic alterations in AIPL1 or NUB1 are associated with retinal degenerative diseases and neurodegenerative α-synucleinopathies [17].

NUB1 overexpression inhibits cell growth [11,12,19],induces cell cycle arrest through the accumulation of p21 and p27 protein [18,19], and affects cancer cell migration, invasion, and epithelial-mesenchymal transition [18]. High NUB1 levels are linked to better outcomes in patients with gastric adenocarcinoma[18]. We examined AIPL1 and NUB1 expression in tumours and correlated it with survival outcomes among breast cancer patients, further investigated the AIPL1-NUB1 system's role in cell cycle regulation and the effects of hypoxia and reoxygenation.

Methods

Patients and breast cancer samples

The study included 122 patients aged 32–80 years with primary infiltrating breast carcinoma diagnosed between 1989 and 1992 at the John Radcliffe Hospital, Oxfordshire, United Kingdom. Eligibility criteria included a histological diagnosis of breast carcinoma, level one or complete axillary lymph node dissection, no distant metastases, and a unilateral tumour. The study protocol was approved by the institutional review board with the ethical approval code C02.216, titled "The Pathobiology of Neoplasia in Human Tissues." Clinicopathological subgroups were analysed according to the Nottingham Prognostic Index (NPI) and all patients were divided into good, moderate, and poor prognostic groups as previously described [20,21]. Tumour samples were collected shortly after surgery and fixed in buffered formalin for 24–48 h at room temperature. Invasive ductal carcinomas were graded using the modified Bloom's grading system, as described by Elston and Ellis [22]. The oestrogen receptor (ER) status was determined using an ELISA assay (Abbott Laboratories).

Oncomine and cBioPortal database analysis

The analysis of the Oncomine database (https://www.oncomine.org/resource/login.html) utilised previously published and open-access microarray data to discern the transcription levels of the NUB1 gene across various types of cancers. Comparisons of NUB1 mRNA expression in clinical cancer tissues and normal controls were calculated using a Student's *t*-test to generate a p-value. The cBioPortal for Cancer Genomics, an open-access resource (http://www.cbioportal.org/), provides visualisation and analysis tools for over 5000 tumour samples from 105 cancer studies within the TCGA pipeline. The search interface, coupled with customised data storage, enables researchers to interactively explore genetic alterations across samples from diverse cancer studies and specific genes. A search for the term 'NUB1′ in the cBioPortal database yielded a cross-cancer summary for further examination.

Cell culture

All cancer cell lines were obtained from the American Type of Cell Collection (ATCC). The HCC1806, MCF-7, MDA-MB-231, SKBR3, BT474, ACHN, 786-O, RCC4, RCC4plusVHL, and T-47D cells were maintained in DMEM supplemented with 10 % (v/v) foetal calf serum (FCS). HCT116 was maintained in McCoy's 5A supplemented with 10 % (v/v) FCS, while Y79 was cultured in RPMI-1640 with 20 % (v/v) FCS. Hypoxic incubations (0.1 % O_2, 5 % CO_2) were performed using an INVIVO2 400 hypoxic workstation (Pro-Lab Diagnostics). Prior to the study and transfections, supernatants of all cell lines were collected and tested with the MycoAlert® mycoplasma detection kit (Lonza Verviers, Belgium) using the MycoAlert® assay control set (Lonza Verviers, Belgium) according to the manufacturer's instructions.

Protocols for immunohistochemistry, Western blot, quantitative real-time PCR, subcellular fractionation, gene silencing by RNA interference, cell cycle analysis using flow cytometry, disulfide bond detection with fluorescein maleimide, and statistical analysis are available in the supplementary materials.

Results

Lower NUB1 mRNA transcription is correlated with poorer breast cancer survival in METABRIC

The prognostic association of AIPL1 and NUB1 gene transcription in various breast cancer molecular subtypes was determined using the METABRIC dataset (Kaplan-Meier survival curves shown in Supp 1). A summary of all the hazard ratios, confidence intervals, and p-values across all molecular subtypes is provided for NUB1 and AIPL1 (Table 1), and for NEDD8 and FAT10 (Table 2). Upregulated AIPL1 was found in the luminal-B subtype. Downregulated NUB1 was found in the ER-negative subtype, HER-2 subtype, enriched HER-2 with ER-negative subtype, and triple-negative subtype (Supp 1). Higher levels of NUB1 mRNA were associated with better overall survival among breast cancer patients over 12 years, but not for AIPL1 (Fig. 1).

Table 1
. Survival curves summary. The survival curve comparing the patients with high and low expression in breast cancer was identified as the threshold of cox p-value <0.05 from METABRIC Kaplan Meier database. The statistically significant hazard rations were bolded in various subtypes of breast cancer identified from the analyses.

Subtype	AIPL1			NUB1		
	Hazard ratio	95 % interval	*p*-value	Hazard ratio	95 % interval	*p*-value
All	1.11	0.97–1.28	0.140	0.83	0.72–0.96	0.010
Basal	0.99	0.71–1.39	0.974	0.76	0.52–1.01	0.061
ER-	0.87	0.66–1.15	0.327	**0.66**	**0.50–0.87**	**0.003**
ER+	1.21	1.03–1.43	0.021	0.89	0.76–1.05	0.186
HER2	0.79	0.55–1.13	0.192	**0.69**	**0.48–0.99**	**0.047**
HER2-	1.16	1.00–1.36	0.054	0.82	0.70–0.96	0.014
HER2+	0.84	0.59–1.19	0.315	0.86	0.61–1.22	0.396
HER2+/ ER-	0.77	0.47–1.26	0.294	**0.63**	**0.38–1.03**	**0.067**
HER2+/ ER+	0.84	0.51–1.38	0.492	1.08	0.66–1.78	0.763
Luminal A	1.15	0.89–1.49	0.291	0.84	0.65–1.09	0.192
Luminal B	**1.42**	**1.09–1.85**	**0.009**	1.02	0.78–1.33	0.886
Normal like	0.85	0.52–1.39	0.526	0.83	0.51–1.36	0.456
ER-/PR-/ HER2-	0.92	0.65–1.31	0.661	**0.67**	**0.47–0.96**	**0.028**

Table 2
. Overall survival summary. The overall survival statistics compare the patients with high and low expression in breast cancer was identified as the threshold of cox p-value <0.05 from METABRIC Kaplan Meier database. HER2 subgroup is non-luminal i.e. HER2 positive but both ER and PR are negative. The statistically significant hazard rations were bolded in various subtypes of breast cancer identified from our analyses.

Subtype	NEDD8			FAT10		
	Hazard ratio	95 % interval	*p*-value	Hazard ratio	95 % interval	*p*-value
All	0.96	0.83–1.10	0.543	0.95	0.82–1.09	0.434
Basal	0.91	0.65–1.27	0.582	**0.65**	**0.46–0.91**	**0.011**
ER-	0.89	0.67–1.17	0.394	**0.72**	**0.55–0.95**	**0.021**
ER+	1.05	0.89–1.24	0.539	1.00	0.85–1.18	0.984
HER2	0.95	0.66–1.36	0.773	0.99	0.69–1.41	0.947
HER2-	1.01	0.87–1.18	0.915	0.94	0.81–1.10	0.428
HER2+	1.12	0.79–1.59	0.517	0.80	0.57–1.14	0.222
HER2+/ER-	1.21	0.73–1.98	0.459	0.76	0.46–1.25	0.275
HER2+/ER+	0.81	0.49–1.34	0.416	0.72	0.43–1.19	0.197
Luminal A	1.05	0.81–1.36	0.693	0.88	0.68–1.14	0.339
Luminal B	0.93	0.71–1.21	0.579	1.07	0.83–1.40	0.596
Normal like	0.79	0.48–1.30	0.354	1.00	0.61–1.63	0.986
ER-/PR-/HER2-	0.75	0.53–1.07	0.111	**0.67**	**0.47–0.95**	**0.025**

AIPL1 mRNA is lower while NUB1 mRNA is concomitantly higher in tumour compared to normal tissue

In Oncomine® (http://www.oncomine.org), we compared gene transcription between tumor and adjacent normal tissue. AIPL1 transcripts were predominantly lower in cancers (24 types of tumors showing down-regulation vs. 3 types of tumors with upregulation compared to their corresponding normal tissue) (Supp 2a, 3a & 3b). Upregulated NUB1 transcripts were found in 37 types of cancer and downregulated in 5 types of cancer. A breast cancer dataset showed a simultaneous decrease in AIPL1 with an increase in NUB1 transcripts compared to its adjacent normal tissue (Supp 2b).

Correlation with pathways in breast cancer

In cBioPortal® (www.cbioportal.org), NUB1 transcripts were co-expressed with cell cycle regulatory proteins. We identified 552, 277, 196, and 349 NUB1-coexpressing genes in datasets such as Breast Cancer [23] (n = 2509), Breast Invasive Carcinoma (TCGA, Provisional) (n = 1105), Breast Invasive Carcinoma [24] (n = 825), and Breast Invasive [25] (n = 817), respectively. A Venn diagram revealed only 28 NUB1-coexpressing genes in common to these datasets (Supp 2c and 4). Reactome® enrichment analysis (https://reactome.org/) indicated that the biological pathways of these 28 genes were predominantly related to the immune response, followed by pathways involved in the cell cycle, apoptosis, signaling, and stress response.

We further evaluated the co-expression of NUB1 transcripts in pathways through Regulome Explorer® (http://www.cancerregulome.org/) analysis using the BRCA 03 Feb 2012 (tumor only) dataset. A scale-independent image showed that CUL1 mRNAs co-expressed with NUB1 mRNA in vivo across this panel of 844 breast cancer samples (Pearson correlation, p = 0.52) (Supp 2d). Both NUB1 and CUL1 transcripts were frequently co-expressed with fatty acid synthase (FAS) and ataxia telangiectasia mutated (ATM) genes in cancer, all of which can be induced by hypoxia.

The AIPL1 protein oligomers have disulphide bonds

To examine protein expression across different cancer cells, we characterised the expression of NUB1, AIPL1, NEDD8, and FAT10 proteins in 11 cancer cell lines from various tumours (kidney, colon, bone, retina, and breast cancer) (Fig. 2a). The Y79 cell line was used as a positive control due to the well-documented expression of AIPL1 and NUB1 in this line [16]. NUB1 protein was detected in all cells except U2OS and SKBR3. AIPL1 protein was observed in both monomer (55 kDa) and dimer (100 kDa) forms. NEDD8 protein was found in the conjugated form with CULs (~70 kDa), while monomers (18 kDa) were present in HCT116, U2OS, HCC1806, and MDA-MB-231 cells. FAT10

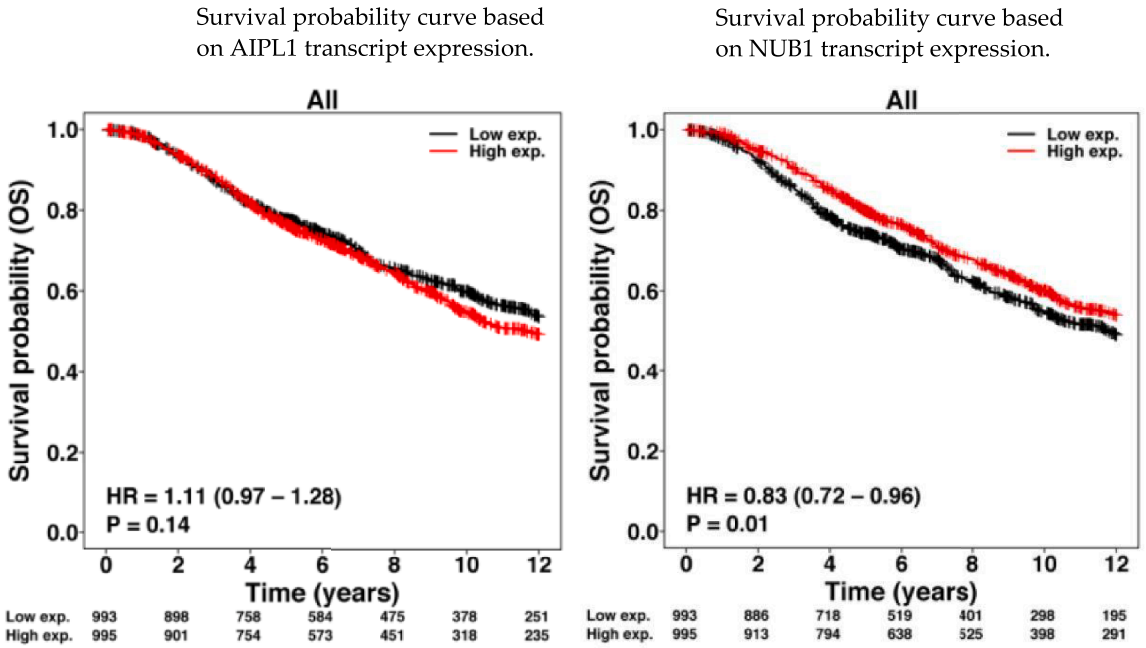

Fig. 1. Survival curves of AIPL1 in different subgroups. The survival curve comparing the patients with high (red) and low (black) expression in breast cancer was identified as the threshold of cox p-value <0.05 from metabric Kaplan Meier database. The survival curve comparing the patients with high (red) and low (black) expression in breast cancer was identified as the threshold of cox p-value <0.05 from METABRIC Kaplan Meier database.

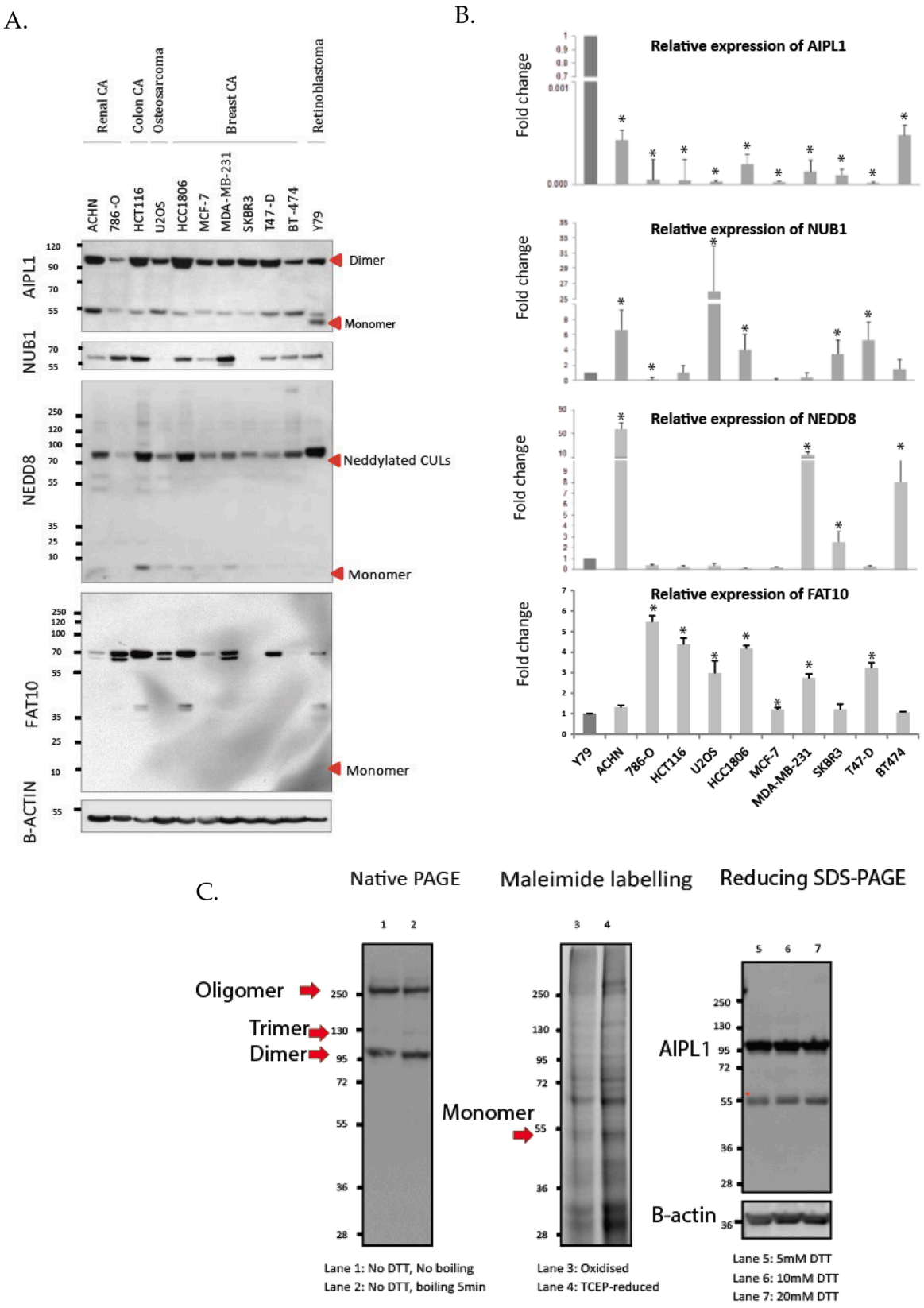

Fig. 2. The screening of protein expressions in cancer cells. (A). Western blot showed the AIPL1, NUB1, NEDD8 and FAT10 proteins in cancer cells derived from varying tissue origins. (B). The relative gene expression AIPL1, NUB1, FAT10 and NEDD8 genes were normalised to β-actin signals. Data shown are means of 3 independent experiments with error bars representing standard deviation. Each bar represents mean ± SEM for each cell lines ($n = 9$). *$p < 0.05$. (C). (Left) Native-PAGE with and without boiling step. (Centre) Maleimide labelling with TCEP treatment. Stronger maleimide signal in lane 4 marks the broken disulphide bonds of proteins. (Right) Immunoblot with titrated DTT.

protein was detected only in the conjugated form, with no monomer observed. The monoclonal mouse anti-AIPL1 antibody (3B4) produced a band on the Western blots at 41.3 kDa, with a slightly higher band was identified around 55 kDa and another larger band at 100 kDa.

Relative transcript expression was analysed in the same cell line panel (Fig. 2b). Using the Y79 cell line as a reference, very low AIPL1 mRNA transcript levels were seen across the cancer cell lines. Greater NUB1 transcript levels were observed in all the cancer cell lines, with U2OS cells showing the highest number of transcripts. NEDD8 mRNA transcript levels were abundant in ACHN, MDA-MB-231, and BT474 cells. The highest amount of FAT10 was found in the 786-O cells.

MDA-MB-231 cell lysates were examined using native-PAGE analysis to confirm that the 100 kDa band was an AIPL1 dimer (Fig. 2c). No AIPL1 monomer was observed under native conditions. Additionally, the maleimide fluorescein method confirmed the presence of disulphide bonds, as the TCEP-reduced sample exhibited a stronger fluorescent signal than the oxidised sample, with a visible band at ~41 kDa. When reoxygenated MDA-MB-231 cells were treated with titrated dithiothreitol (DTT), AIPL1 monomers increased, while the dimer with strong bonds resisted DTT cleavage.

Subcellular localisation and migration of AIPL1 and NUB1 proteins upon hypoxia

Immunohistochemistry staining was used to determine the distribution of AIPL1, NUB1, and NEDD8 proteins under non-stressed conditions (not shown). AIPL1 protein was observed predominantly in the cytoplasm, with lesser amounts found in the nucleus. ACHN and BT474 cells expressed the least AIPL1 protein. All cells showed positive staining for NUB1 protein, except for U2OS. NEDD8 protein was abundantly present in both the nucleus and the cytoplasm of all cell lines. In contrast, FAT10 protein was detected in most cells, but was absent in HCT116, T47-D, and BT474 cells.

To examine how NUB1 protein responds in the ER-negative subtype under stress, MDA-MB-231 was selected due to its invasive nature and treatment difficulty. The cell line was subjected to reoxygenation after severe hypoxic conditions (0.1 % O_2 for 48 h) (Fig. 3a). AIPL1 oligomers did not change, but increased levels of neddylated cullins (NEDD8CULs) and NUB1 proteins were observed as early as 5 min after reoxygenation. The subcellular localisation of AIPL1 and NUB1 proteins was studied under both hypoxic and reoxygenated conditions (Fig. 3b). In normoxia, AIPL1 protein was predominantly monomeric, with minimal dimers present in the nucleus. However, in hypoxic conditions and upon reoxygenation, both monomers and dimers accumulated in the cytoplasm, while nuclear AIPL1 dimers were depleted. More nuclear AIPL1 monomers were observed in hypoxia and fewer upon reoxygenation. NUB1 protein levels increased in the cytoplasm under normoxia. After 24 h of hypoxia, both cytoplasmic and nuclear NUB1 levels rose. After 48 h of hypoxia, NUB1 protein progressively accumulated in the nucleus, with reduced levels in the cytoplasm. These findings support the established role of AIPL1 as a protein that facilitates the translocation of NUB1 into the nucleus.

NUB1 could protect cells from apoptosis through VHL in hypoxia

The role of NUB1 and VHL proteins was examined in RCC4 cell lines. In hypoxia, knockdown of NUB1 in RCC4plusVHL cells reduced the number of cells in the G0/G1 phase. Specifically, there was a decrease in cells in the G2/M phase (25.7 % ± 2.5 vs 36.2 % ± 3.1; $p < 0.001$) and an increase in cells in the sub-G1 phase (20.2 % ± 0.7 vs 9.0 % ± 2.16; $p < 0.01$) (Fig. 5a). The levels of HIF1α and VHL proteins were assessed in RCC4 and RCC4plusVHL cells, with NUB1 knockdown resulting in decreased VHL levels in RCC4plusVHL cells (Fig. 5b). Increased presence of cleaved PARP under hypoxic conditions in RCC4plusVHL cells suggested that cell death was due to apoptosis, and this was more pronounced in the absence of NUB1. Additionally, the p21 protein level

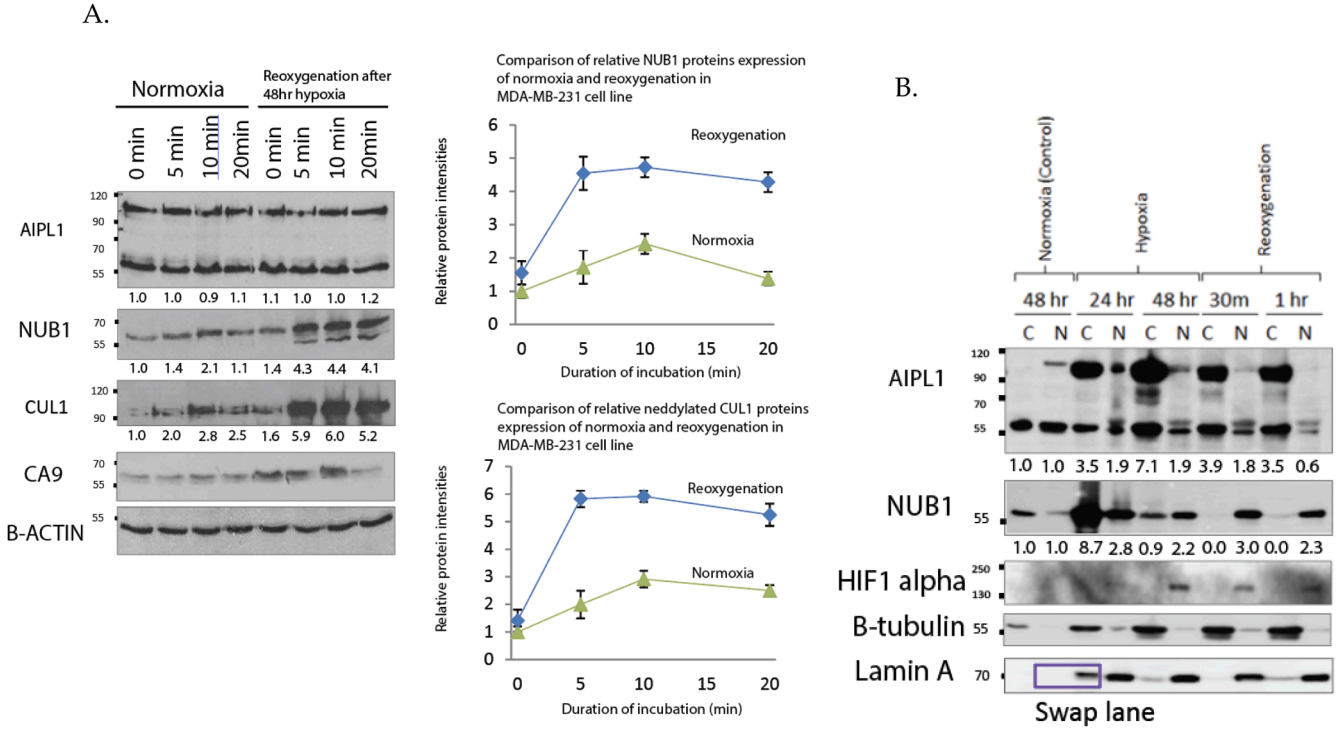

Fig. 3. Time course experiment of reoxygenated MDA-MB-231 (A). MDA-MB-231 cells were incubated in hypoxia and reoxygenated. Lysates were collected according to the time point. The levels of proteins were compared to the normoxic cells. Both NUB1 and NEDD8-CULs proteins were significantly different than the normoxic cells. Abbr CA9: carbonic anhydrase 9. Cytoplasmic AIPL1 dimers drove NUB1 protein shuttling into the nucleus. (B) MDA-MB-231 lysates were subjected to subcellular fractionation, cytoplasmic and nuclear fractions were analysed by immunoblotting. β-tubulin and lamin A were used as controls. Endogenous proteins were quantified and values normalised to tubulin or lamin A.

increased following NUB1 knockdown, indicating that NUB1 might protect cells from apoptosis through VHL under hypoxic conditions. In RCC4 cell cycle analysis, a significantly higher percentage of sub-G1 cells was detected in NUB1 knockdown cells both in normoxia (14.71 % ± 3.21 vs 48.73 % ± 7.56, $p < 0.05$) and hypoxia (11.12 % ± 3.78 vs 32.89 % ± 2.11, $p < 0.05$), whereas the percentage of cells in the G0/G1 phase decreased. No accumulation of cleaved PARP or p21 was observed following NUB1 silencing, suggesting that these effects were VHL-mediated.

To test whether NUB1 influences the activity of CUL2-based complexes, HIF1α and VHL levels were measured in a renal cell carcinoma cell line. The level of HIF1α in hypoxia in the NUB1 knockdown RCC4 group was nearly threefold greater than in the control siRNA group (1.13 ± 0.51 vs 3.59 ± 0.36-fold, $P < 0.001$). The VHL level dropped following NUB1 knockdown in RCC4plusVHL cells under hypoxia (0.90 ± 0.16 vs 0.42 ± 0.10; $P < 0.001$) (Fig. 6a). To determine whether the roles of NUB1 were VHL-dependent, cell cycle profiles of cells exposed to normoxic or hypoxic conditions were examined (Fig. 6b). In RCC4 cells, a greater percentage of sub-G1 cells was detected in NUB1 siRNA-treated samples under hypoxia compared to non-targeting controls. Increased cell death was observed in the hypoxic, NUB1 siRNA-treated group, suggesting a role for NUB1 in protecting cells from hypoxia-induced replication stress. HIF1α was upregulated in NUB1 knockdown cells. This cell cycle analysis highlights a potential role for NUB1 in protecting cells from cell death responses under severe hypoxic conditions.

To explore the specific contributions of VHL to tumour suppression and understand the interplay between CUL1 and CUL2, we examined the effects of NUB1 in RCC4plusVHL and RCC4 cells (Fig. 7a). Depletion of NUB1 upregulated p27 protein in both RCC4 and RCC4plusVHL cells. The upregulation of HIF1α was observed only in RCC4 cells under normoxia, hypoxia, and after reoxygenation. In RCC4plusVHL cells, NEDD8 levels increased under normoxia in the absence of NUB1, while limited NEDD8 protein was seen in RCC4 cells. However, a higher level of NEDD8-CUL2 was observed in RCC4 cells and increased further after NUB1 silencing. NUB1 silencing also increased p27 protein in both cell lines. The increase in p27 and HIF1α following NUB1 depletion was seen in both cell lines, suggesting that HIF1α could be stabilised via a non-ubiquitin regulated mechanism (Fig. 7a). Additionally, endogenous HIF1α was found to be neddylated or fat10ylated in MDA-MB-231 cells (Fig. 7b).

Lower NUB1 protein expression is associated with poorer breast cancer survival

The NUB1 antibody, clone 4H2, was validated for clinical implementation as a protein biomarker using the immunohistochemistry method (Supp 5). The protein retained its antigenicity in archival tissues, with no systematic loss of antigenicity observed, as indicated by the reliable staining patterns in the tested breast cancer specimens. Among the 152 primary breast cancer tumours collected in the tissue microarray (TMA), 122 tumour cores (80 %) were interpretable with associated survival information. Uninterpretable spots were either due to tissue loss on the TMA or a lack of tumour cells in the spot.

Immunohistochemical staining of the breast cancer tissue microarray with NUB1 revealed cytoplasmic and/or nuclear localisation. Compared to ER-negative patients, a similar distribution pattern was observed in ER-positive patients, but with a stronger intensity (3+) score for NUB1. The highest frequency of cytoplasmic staining in ER-negative patients was mild (1+), while the highest frequency of cytoplasmic staining in ER-positive patients was moderate (2+). A total of 100 tumours (80 %) showed positive NUB1 cytoplasmic staining, and 66 tumours (23.1 %) exhibited positive NUB1 nuclear staining. A subset of 99 tumours was positive for both NUB1 cytoplasmic and nuclear staining (80 %). ER immunoreactivity was evaluable in 122 (96.1 %) cases and was positively scored in 99 (78 %) cases using intensity scores of 2+ and 3+ to indicate ER protein overexpression. Tumours with ER intensity scores of 0 or 1+ were assessed as negative. ER expression was analysed in relation to clinicopathological criteria (Table 3), showing a significant association of ER negativity with positive node status ($p < 0.01$), ER negativity with the highest histological grade tumours ($p < 0.01$), and ER negativity with larger tumour size ($p < 0.01$).

A strong correlation was noted between the nuclear NUB1 immunohistochemical score (IPS) and the cytoplasmic NUB1 IPS ($\rho = 0.76$, $p < 0.01$) (Fig. 8a). Cytoplasmic NUB1 was significantly higher in ER-positive tumours, with a mean IPS of 138 (95 % CI: 121–155), compared to a mean IPS of 86 (95 % CI: 53–120) in ER-negative patients ($\rho = 0.02$). Nuclear NUB1 staining in both groups did not show any significant difference. ER-positive tumours exhibited increased cytoplasmic NUB1 (Fig. 8b). Although the underlying mechanism remains unknown, a lower cytoplasmic NUB1 level in ER-negative tumours is associated with clinical aggressiveness. A 16-year follow-up Kaplan-Meier survival curve was generated based on the subcellular localisation in all patients (Fig. 8c). No significant difference in overall survival was predicted by nuclear NUB1 staining. However, lower cytoplasmic NUB1 staining was significantly correlated with poorer overall survival but not with relapse-free survival. In multivariate analysis, a lower level of cytoplasmic NUB1 in ER-negative patients was related to significantly poorer survival (Fig. 8d). Significantly lower cytoplasmic IPS was found in premenopausal patients. Additionally, nuclear NUB1 scores were significantly lower in HER2-positive and premenopausal samples (Table 4).

Discussion

A meta-analysis of gene-specific transcriptomic microarray data on HSPs identified AIPL1 as a new biomarker, [26] highlighting its role in protein folding, although it remains underexplored in cancer. AIPL1 protein negatively regulates NUB1 protein trafficking across the nuclear membrane in a retinal model [16]. In cancer, AIPL1 transcript levels decreased (>0.25 $\log_2$ fold change), while NUB1 was upregulated (>0.5 $\log_2$ fold change). The opposite in vivo transcript expressions suggest a reciprocal regulatory mechanism. CUL1 was most frequently co-expressed with NUB1 (Supp 4) in pathways such as T-Cell receptor signalling, interferon (IFN), and interleukin regulation. NUB1, involved in the immunity pathway, can be induced by IFNβ [19].

AIPL1 protein, in its multimeric forms, forms dimers in the cytoplasm during hypoxia, whereas NUB1 localises in the nucleus, appearing as oligomers under physiological conditions.

Table 3
. Clinicopathological variables according to ER status. Grade I patients showed significantly more frequent to the rest of the grades in ER positive patients. Positive nodal status was found significantly in ER negative patients. Significantly more patients at > 50 years old were found in ER positive.

	ER-negative	ER-positive	*p*-value	Overall
Total	23	99		122
c-erbB2 receptor status				
Negative	6	50	0.092	56
Postive	7	17		24
Node status				
Negative	7	58	0.009*	65
Positive	16	38		54
Histologic grade				
Grade I	0	18	0.0001*	18
Grade II	2	50		52
Grade III	15	17		32
Age				
< 50 years	7	19	0.236	26
≥ 50 years	16	80		96
Median (range)	53 (26–90)	59 (34–83)		58 (26–90)
Tumour size				
≤ 2 cm	4	47	0.008*	51
> 2 cm	19	52		71
Median (range)	3.7 (0–8.0)	2.36 (0–7.3)		2.5 (0–8.0)

Table 4
. Summary of overall survival analysis based on the mean IPS.

Variable	Events	Cytoplasmic			nuclear		
		Mean IPS	95 % confidence interval	*P*	Mean IPS	95 % confidence interval	*P*
Age, yr	116		−0.011, −0.26	0.079[a]		−0.12, 0.25	0.065[a]
Size, cm							
≤2	72	124	105–143		190	157–222	
>2	41	139	114–164	0.371	177	152–201	0.534
Lymph nodes							
Uninvolved	59	137	117–157		190	164–216	
Involved	54	115	92–138	0.172	164	134–194	0.195
Grade							
1	15	143	104–183		206	146–265	
2	51	133	111–155	Ns	180	152–208	ns
3	33	103	74–133	Ns	113	113–189	ns
Histology							
Ductal	94	122	104–183		172	150–194	
Lobular	14	133	111–155	Ns	222	179–265	ns
Other	8	103	74–133	Ns	186	98–274	ns
ER							
Negative	**21**	**86**	**53–120**		147	95–200	
Positive	**90**	**138**	**121–155**	**0.017***	191	170–211	0.166
HER2							
Negative	**52**	132	109–156		**189**	**160–219**	
Positive	**21**	104	64–144	0.300	**138**	**90–187**	**0.043***
Menopausal status							
Pre	**25**	**95**	**58–132**		**138**	**160–183**	
Post	**91**	**135**	**119–151**	**0.022***	**190**	**169–211**	**0.043***
EGFR							
negative	42	130	105–155		183	150–215	
positive	44	145	125–166	0.437	216	192–240	0.143

* Significant *p*-value.
[a] Pearson correlation analysis.

NUB1 proteins responded to low oxygen tension. Upon reoxygenation, NUB1 and neddylated CULs proteins were upregulated within 5 min in MDA-MB-231 (Fig. 4a). NUB1 knockdown induced cell cycle arrest with reduced sub-G1 and S-phase populations, aligning with a previous study showing that NUB1 overexpression promotes S-phase transition in renal cells[19]. Depleted NUB1 cells accumulated p27 and p21 protein, inhibiting ubiquitin-mediated degradation. [19]. Nuclear NUB1 found in reoxygenated cells could not sustain cells in the sub-G1 state, unlike its cytoplasmic counterpart.

Folded and unfolded AIPL1 were found in monomer and dimer forms (Fig. 2c). TCEP treatment did not completely diminish the fluorescein signal, indicating multiple disulphide bonds. Native and reduced forms of AIPL1 confirmed the presence of AIPL1 dimers with multiple cysteine-cysteine disulphide bonds.

NUB1 and CUL1 proteins regulate the cell cycle. Overexpressed NUB1 formed redundant aggregates [10] while AIPL1 suppressed inclusion body formation [10]. NUB1 knockdown slowed growth in MDA-MB-231 and T-47D cells under hypoxia. Folded AIPL1 in the cytoplasm chaperoned NUB1, facilitating its translocation into the nucleus during hypoxia and reoxygenation, showcasing their oxygen-sensing capabilities. The nuclear distribution of NUB1 also influenced cancer cell fate [10].

NUB1 and VHL proteins protect RCC4 cells from apoptosis in chronic severe hypoxia. NUB1's protective role involved non-apoptotic pathways, as evidenced by the presence of non-cleaved PARP when NUB1 was absent during cell death (Fig. 5). In the absence of VHL, NUB1 silencing induced G_0/G_1 arrest in both hypoxia and normoxia.

Depletion of NUB1 in RCC4 cells led to an upregulation of HIF1α, p21, and p27 proteins. However, this upregulation of HIF1α occurred only in RCC4plusVHL (Fig. 7a). NUB1 protein potentially caused the degradation of free neddylated CUL2. Despite this, the neddylated CUL2-based ubiquitin E3 ligase remained in the RBX1 complex. CUL2-based ubiquitin E3 ligases competitively bound to RBX1, resulting in decreased engagement with CUL1-based ubiquitin E3 ligases (Supp 6a & 6b). Consequently, there was increased degradation of p27 and p21 proteins.

CULs serve as substrates of neddylation and neddylated CUL1 engages with the ubiquitin E3 ligase, leading to the degradation of p21 and p27 proteins [27]. NUB1 depletion resulted in reduced levels of neddylated CUL1 (Fig. 7a) and NEDD8, [19] leading to an accumulation of p27 and p21 proteins. This was further confirmed by MLN4724 treatment, a neddylation inhibitor, which also upregulated p21 and p27 in an additive manner. As free CUL1 proteins become neddylated, the resulting neddylated CUL1 protein then interacts with the ubiquitin E3 ligase, leading to an enhanced degradation of p27 and p21. Inhibition of neddylation resulted in an accumulation of p21 and p27 proteins during G_1 cell cycle arrest, Consistent with NUB1 silence-induced accumulation.

RCC4, a model for studying the interplay between NUB1 and VHL proteins in hypoxia responses, showed reduced VHL protein upon NUB1 knockdown in RCC4plusVHL cells. Hypoxia under these conditions resulted in increased p21 protein and apoptotic cells (Fig. 6c). NUB1 protein facilitated S-phase transition during hypoxia, preventing cell cycle arrest and senescence. In the absence of VHL, NUB1 knockdown caused RCC4 cells to lean towards necrotic cell death, lacking non-cleaved PARP and G0/G1 cell cycle arrest markers. VHL determined cell fate between apoptosis and necrosis during NUB1 depletion. VHL protein protected UV-treated cells from apoptosis, which resulted from perturbed cell cycle checkpoints during DNA damage repair [28].

VHL, a component of the CUL2-based ubiquitin E3 ligase, competitively occupies RBX1, indirectly deactivating CUL1-based ubiquitin E3 ligase (Supp 6a) [28]. This leads to the accumulation of p21 and p27 proteins in cells. The activity indicator of the CUL2-based ubiquitin E3 ligase, HIF1α levels, was lower (Supp 6b) in RCC4plusVHL cells, suggesting a more active CUL2-based ubiquitin E3 ligase compared to CUL1. In VHL-null RCC4 cells, both p21 and p27 accumulated (Fig. 7a), indicating that RBX1 did not bind to CUL1-based ubiquitin E3 ligase under stress.

HIF1α stabilised with NUB1 silencing, being covalently modified by NEDD8 and FAT10 (Fig. 7b). Endogenous neddylated HIF1α was further

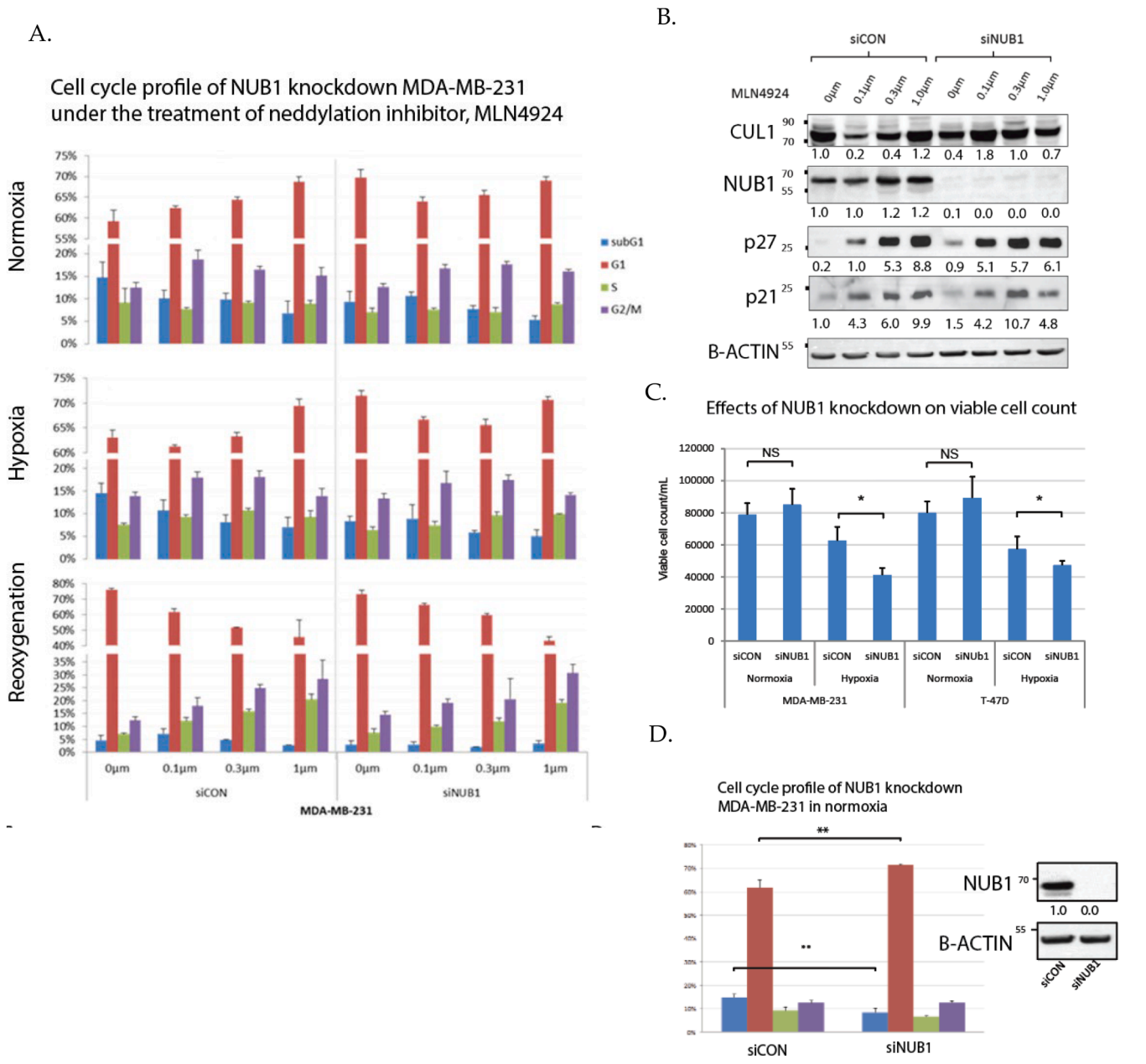

Fig. 4. Knockdown of NUB1 and cell cycle analysis (A). Cell cycle analysis was performed to examine the cell cycle distribution in each group, and quantification. Data represented as mean±*s*.d; *$p < 0.05$. NUB1 silencing enhances neddylation inhibition effects onto p27 (but not p21) protein levels in normoxia (B). MDA-MB-231 cells were treated with siRNA and titrated MLN 4924 for 48hr in normoxia. This experiment was performed twice. Densitometry (indicated by numbers beneath the immunoblot) was performed using ImageJ. The effect of NUB1 knockdown condition to cancer cell growth (C). Viable cell numbers were calculated after siNUB1 transient transfection in 11 normoxia (48 h, 21 % O2) and chronic severe hypoxia (48 h 0.1 % O2). Cell cycle profiles of NUB1 knockdown in MDA-MB-231 cells (D). Bars, mean+ *s*.e.m.; $n = 9$; *$p < 0.05$.

stabilised in hypoxia [20]. VHL protein targets hydroxylated HIF1α, forming the CUL2-based ubiquitin E3 ligase complex that ubiquitinates HIF1α [29], which is reported to stabilise HIF1α via VHL-mediated ubiquitination [20]. Thus, HIF1α regulation involves NEDD8 in VHL-defective cells.

TMA analysis correlated survival with NUB1 proteins in breast cancer patients. Nuclear NUB1 IPS strongly correlated with cytoplasmic NUB1 IPS (Fig. 8a). Depletion of NUB1 and ER proteins resulted in significantly lower survival rates.

Low expression of NUB1 proteins predicted poorer overall survival due to metastasis-induced death. Low cytoplasmic NUB1 protein reflects a reduced capacity of cancer cells to overcome challenges such as hypoxia and DNA damage, inhibiting downstream apoptotic pathways and allowing tumour proliferation and distant metastasis. NUB1 expression is associated with a better outcome, though NUB1 immunostaining in ER-negative patients indicates a poor prognosis. High NUB1 expression is linked to cancer progression from normal cells, suggesting a non-aggressive cancer pathway.

Strategies targeting NUB1 for Huntington's disease treatment may also prevent distant metastasis [30,31]. Lacking a receptor or enzymatic function, NUB1 relies on interaction with other proteins. Focusing on NUB1's adaptor function and its synergy with the neddylated CULs pathway could unlock its potential functions.

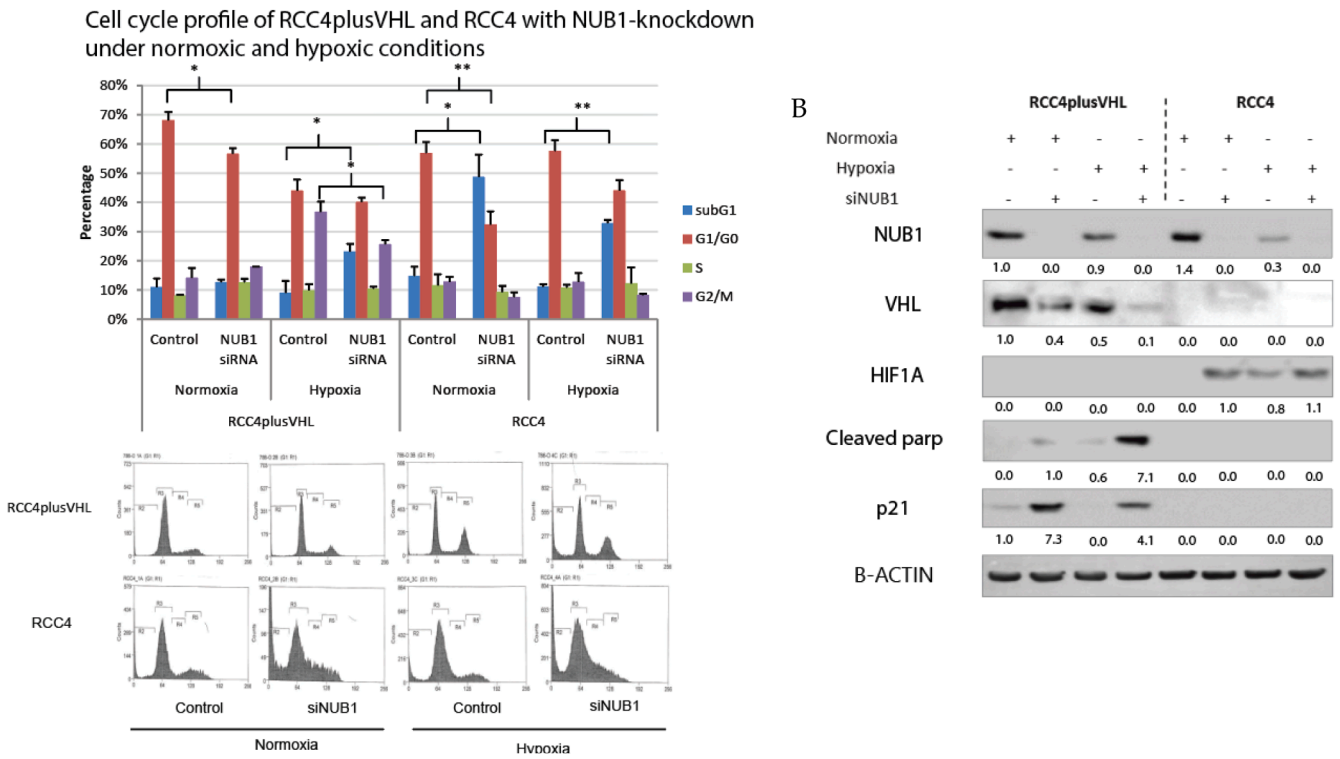

Fig. 5. Cell cycle analysis in NUB1 knockdown MDA-MB-231 in normoxia (A). The cells were harvested, stained with propidium iodide and subjected to FACs analysis. Cell cycle profile of each experiment group. Data shown are means of 3 independent experiments with error bars representing standard deviation. Each bar represents mean ± SEM for each cell line ($n = 9$). * significant at $p < 0.05$; ** significant at $p < 0.005$. Effect of NUB1 knowckdown on the cell cycle of RCC4plusVHL and control cells under normoxic and hypoxic conditions (B). Immunoblotting of p21 (G1/G0) marker and apoptosis marker, PARP under the different experimental conditions.

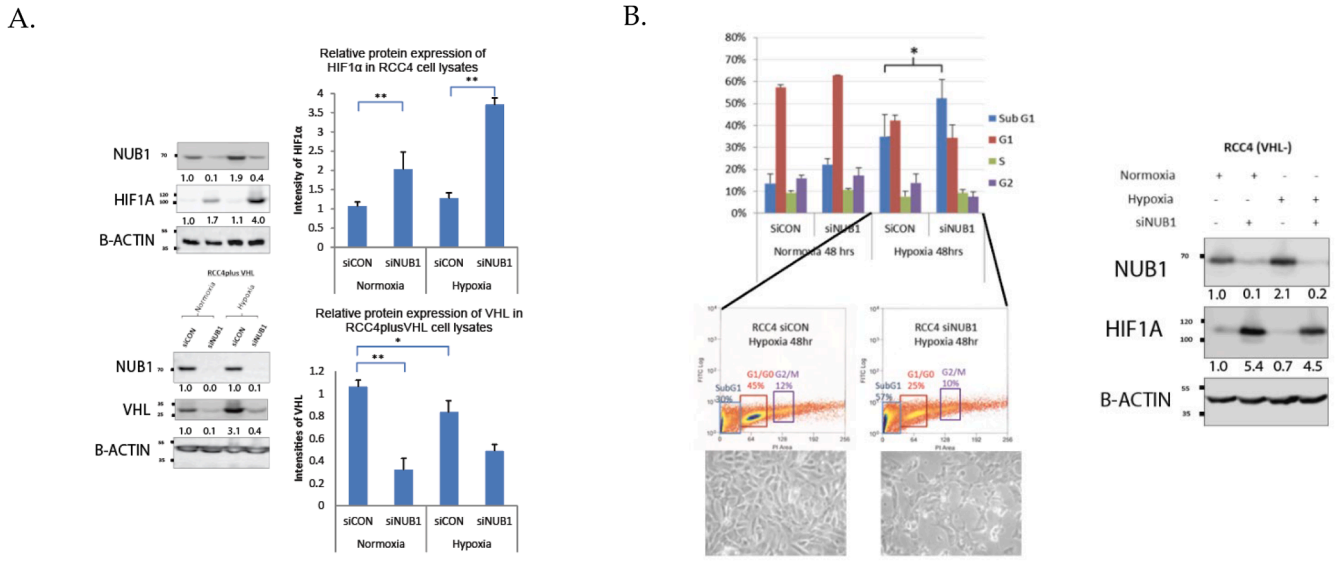

Fig. 6. NUB1 knockdown upregulates HIF1α and downregulates VHL (A); Cell cycle analysis on the NUB1 knowckdown effect in RCC4 cells under normoxic and hypoxic conditions (B). RCC4plusVHL and RCC4 cells were transfected with 100 pmol siRNA as indicated. The amount of HIF-1α was calculated as the difference between siCon and siNUB1 groups. Cell lines were transfected with siNUB1 and incubated for 48 h. NUB1 knockdown of hypoxic RCC4 showed significant cell death compared to the control. HIF1α was up-regulated in NUB1 knockdown cells. Bars represent the means ± *S*.D. of 3 independent biological replicates. * significant at $p < 0.05$; ** significant at $p < 0.005$.

Conclusion

In the multivariate analysis of prognostic clinicopathological parameters, NUB1 was identified as an independent marker for overall survival in breast cancer patients. Low cytoplasmic expression of NUB1 was significantly linked to a worse prognosis in ER-negative breast cancer cases. This suggests that low cytoplasmic NUB1 expression is a valuable prognostic biomarker for predicting tumour progression and poorer overall survival. Reduced levels of NUB1 can lead to tumour growth arrest, proliferation, and distant metastasis by inducing CUL1

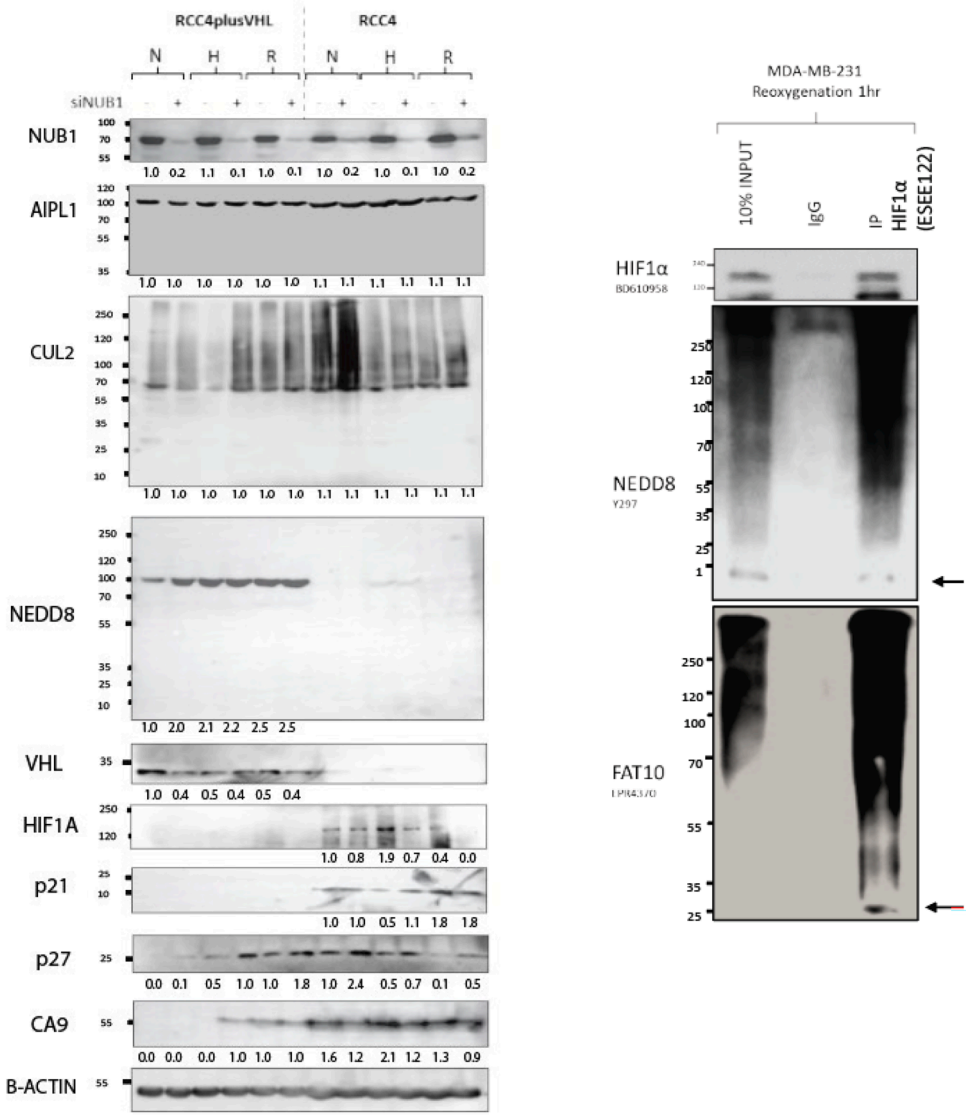

Fig. 7. Depletion of NUB1 upregulated HIF1α and p27 proteins (A); NEDD8 and FAT10 signals detected in endogenous HIF1α (B). The lysates from RCC4plusVHL and RCC4 cells were transfected with siNUB1 and underwent normoxia, hypoxia for 48 hr and reoxygenated 24 h. The cell lysates were analysed by Western blotting using antibodies, and by densitometric analysis. *N*=normoxia, H: hypoxia, R: reoxygenation. Densitometry was quantified using ImageJ and the figure indicated the relative densities to a band equal to 1.0. Cells lysate from MDA-MB-231 cells were immunoprecipitated with control IgG or HIF1α antibodies, and subsequently immunoblotted with the indicated antibodies. Input levels of HIF1α protein are as shown.

neddylation, which in turn causes the accumulation of p21 and p27.

Institutional Review Board Statement

The study protocol was approved by the institutional review board. The ethical approval code used for this study is C02.216 "The pathobiology of neoplasia in human tissues".

Informed consent statement

Not applicable.

Funding

This research was funded by Ministry of Higher Education (MOHE) under the Fundamental Research Grant Scheme (FRGS) with reference number FRGS/1/2019/SKK15/USIM/03/1.

CRediT authorship contribution statement

Ka-Liong Tan: Writing – original draft, Visualization, Project administration, Funding acquisition, Formal analysis, Conceptualization. **Syed Haider:** Supervision, Methodology, Data curation. **Christos E. Zois:** Supervision, Project administration, Methodology, Investigation, Conceptualization. **Jianting Hu:** Project administration, Methodology, Investigation, Data curation. **Helen Turley:** Visualization, Validation, Resources, Formal analysis. **Russell Leek:** Software, Resources. **Francesca Buffa:** Software, Formal analysis, Data curation. **Oreste Acuto:** Validation, Investigation. **Adrian L. Harris:** Writing – review & editing, Investigation, Conceptualization. **Francesco Pezzella:** Writing – review & editing, Supervision, Resources, Funding acquisition.

Declaration of competing interest

The authors declare no competing interest. The sponsors had no role in the design, execution, interpretation, or writing of the study.

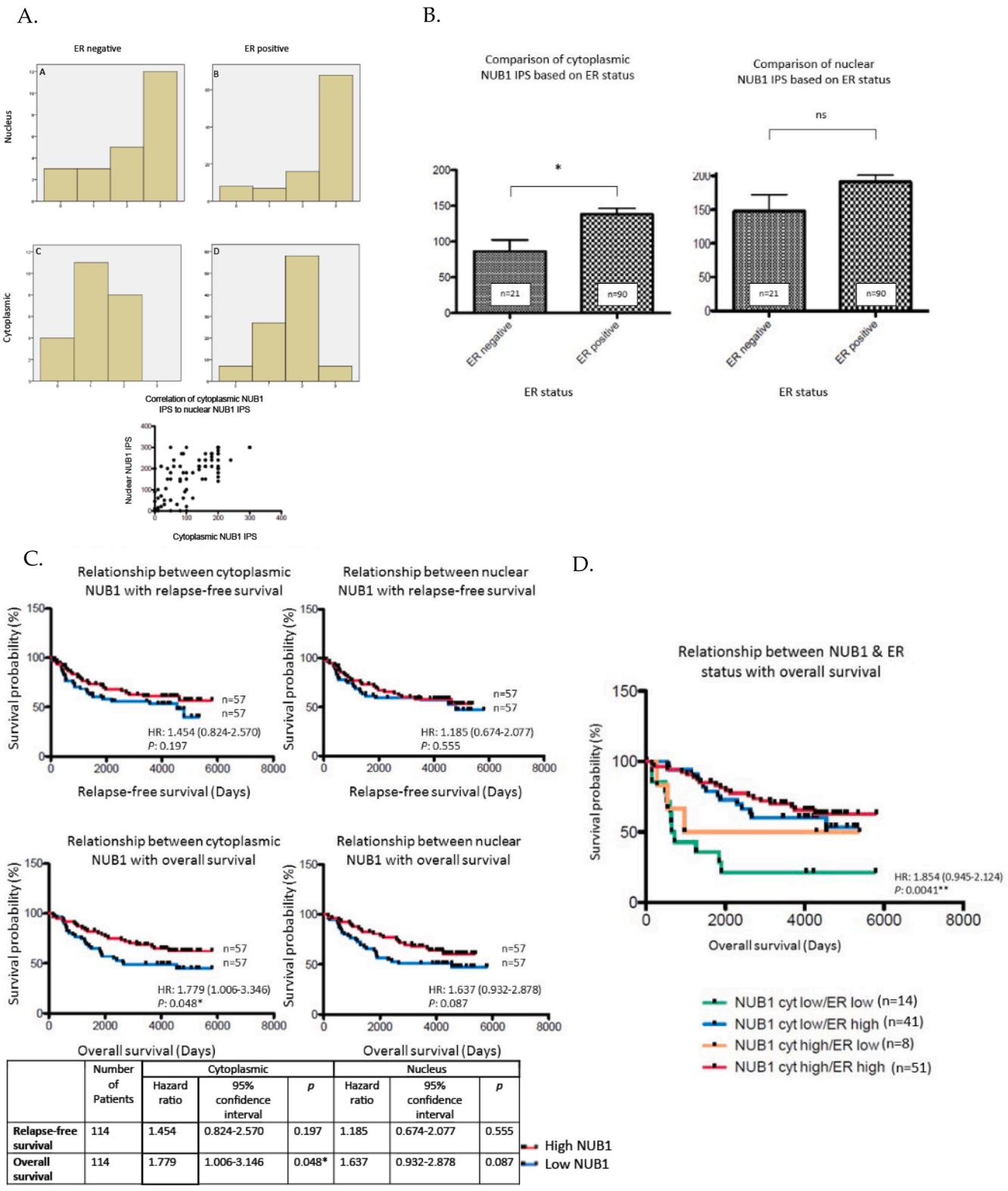

	Number of Patients	Cytoplasmic			Nucleus		
		Hazard ratio	95% confidence interval	p	Hazard ratio	95% confidence interval	p
Relapse-free survival	114	1.454	0.824-2.570	0.197	1.185	0.674-2.077	0.555
Overall survival	114	1.779	1.006-3.146	0.048*	1.637	0.932-2.878	0.087

Fig. 8. Distribution of NUB1 immunohistochemical staining scores in primary breast cancer (A); A. NUB1 nuclear staining scores in ER- subgroup; B, NUB1 nuclear staining scores in ER+ subgroup C, NUB1 cytoplasmic staining scores in ER- subgroup; D, NUB1 cytoplasmic staining scores in ER+ subgroup. Correlation of NUB1 cytoplasmic IPS with nuclear IPS, $r = 0.76$ (0.67–0.83). Relationship between ER status and NUB1 localisation (B). Bar charts according to ER status and the subcellular localisation of NUB1 measured as an IPS. (a)Distribution of cytoplasmic NUB1 IPS and medians according to ER-negative and ER-positive breast cancers, with patient numbers shown. (b) Nuclear NUB1 IPS and medians according to ER status, and numbers of patients. P values indicate significance. Relationship between high/low NUB1 subcellular localisation and overall survival/ relapse free survival (C); Overall survival curves were plotted according to ER and NUB1 status. Relationship between ER and prognosis in breast cancer patients using the log-rank test (D). Relapse-free survival curves according to HER-2 expression.

Data availability

All data are incorporated into the article and its online supplementary material.

Acknowledgments

K. Tan was supported by graduate fellowship under Ministry of Higher Education, Malaysia.

Supplementary materials

Supplementary material associated with this article can be found, in the online version, at doi:10.1016/j.tranon.2024.102106.

References

[1] S.K. Calderwood, Molecular cochaperones: tumor growth and cancer treatment, Scientifica. (Cairo). 2013 (2013) 217513.
[2] A. Ramasamy, Increasing Statistical Power and Generalizability in Genomic Microarray Research, Oxford, Oxford, 2009, p. 152.
[3] J. Hu, et al., TRAP1 is involved in cell cycle regulated by retinoblastoma susceptibility gene (RB1) in early hypoxia and has variable expression patterns in human tumors, J. Can. Res. Update. 2 (3) (2013) 194–210.
[4] C.F. Chen, et al., A new member of the hsp90 family of molecular chaperones interacts with the retinoblastoma protein during mitosis and after heat shock, Mol. Cell. Biol. 16 (9) (1996) 4691–4699.
[5] H. Tsuchiya, T. Iseda, O. Hino, Identification of a novel protein (VBP-1) binding to the von Hippel-Lindau (VHL) tumor suppressor gene product, Cancer Res. 56 (13) (1996) 2881–2885.
[6] K. Basso, et al., Reverse engineering of regulatory networks in human B cells, Nat. Genet. 37 (4) (2005) 382–390.
[7] L. Dyrskjot, et al., *Gene expression in the urinary bladder: a common carcinoma* in situ *gene expression signature exists disregarding histopathological classification*, Cancer Res. 64 (11) (2004) 4040–4048.
[8] M.E. Lenburg, et al., Previously unidentified changes in renal cell carcinoma gene expression identified by parametric analysis of microarray data, BMC Cancer 3 (2003) 31.
[9] S. Ramaswamy, et al., Multiclass cancer diagnosis using tumor gene expression signatures, Proc. Natl. Acad. Sci. U.S.A. 98 (26) (2001) 15149–15154.
[10] J. van der Spuy, M.E. Cheetham, The Leber congenital amaurosis protein AIPL1 modulates the nuclear translocation of NUB1 and suppresses inclusion formation by NUB1 fragments, J. Biol. Chem. 279 (46) (2004) 48038–48047.
[11] T. Kamitani, et al., Targeting of NEDD8 and its conjugates for proteasomal degradation by NUB1, J. Biol. Chem. 276 (49) (2001) 46655–46660.
[12] K. Kito, E.T. Yeh, T. Kamitani, NUB1, a NEDD8-interacting protein, is induced by interferon and down-regulates the NEDD8 expression, J. Biol. Chem. 276 (23) (2001) 20603–20609.
[13] K. Tanji, T. Tanaka, T. Kamitani, Interaction of NUB1 with the proteasome subunit S5a, Biochem. Biophys. Res. Commun. 337 (1) (2005) 116–120.
[14] M. Groettrup, et al., Activating the ubiquitin family: UBA6 challenges the field, Trend. Biochem. Sci. 33 (5) (2008) 230–237.
[15] M.M. Sohocki, et al., Mutations in a new photoreceptor-pineal gene on 17p cause Leber congenital amaurosis, Nat. Genet. 24 (1) (2000) 79–83.
[16] J. van der Spuy, et al., The Leber congenital amaurosis gene product AIPL1 is localized exclusively in rod photoreceptors of the adult human retina, Hum. Mol. Genet. 11 (7) (2002) 823–831.
[17] K. Tanji, et al., NUB1 suppresses the formation of Lewy body-like inclusions by proteasomal degradation of synphilin-1, Am. J. Pathol. 169 (2) (2006) 553–565.
[18] D. Zhang, et al., Overexpression of negative regulator of ubiquitin-like proteins 1 (NUB1) inhibits proliferation and invasion of gastric cancer cells through upregulation of p27Kip1 and inhibition of epithelial-mesenchymal transition, Pathol. Res. Pract. 216 (8) (2020) 153002.
[19] T. Hosono, et al., NUB1, an interferon-inducible protein, mediates anti-proliferative actions and apoptosis in renal cell carcinoma cells through cell-cycle regulation, Br. J. Cancer 102 (5) (2010) 873–882.
[20] J.H. Ryu, et al., Hypoxia-inducible factor alpha subunit stabilization by NEDD8 conjugation is reactive oxygen species-dependent, J. Biol. Chem. 286 (9) (2011) 6963–6970.
[21] A. Saha, R.J. Deshaies, Multimodal activation of the ubiquitin ligase SCF by Nedd8 conjugation, Mol. Cell. 32 (1) (2008) 21–31.
[22] C.W. Elston, I.O. Ellis, Pathological prognostic factors in breast cancer. I. The value of histological grade in breast cancer: experience from a large study with long-term follow-up, Histopathology 19 (5) (1991) 403–410.
[23] B. Pereira, et al., The somatic mutation profiles of 2,433 breast cancers refines their genomic and transcriptomic landscapes, Nat. Commun. 7 (2016) 11479.
[24] Anon, TAGCN, Comprehensive molecular portraits of human breast tumours, Nature 490 (7418) (2012) 61–70.
[25] G. Ciriello, et al., Comprehensive molecular portraits of invasive lobular breast cancer, Cell 163 (2) (2015) 506–519.
[26] Adaikalavan, R., *Increasing Statistical Power and Generalizability in Genomics Microarray research.*, in *Nuffield division of Clinical Laboratory Sciences*. 2009., Oxford.
[27] K. Wu, A. Chen, Z.Q. Pan, Conjugation of Nedd8 to CUL1 enhances the ability of the ROC1-CUL1 complex to promote ubiquitin polymerization, J. Biol. Chem. 275 (41) (2000) 32317–32324.
[28] A.R. Schoenfeld, et al., The von Hippel-Lindau tumor suppressor gene protects cells from UV-mediated apoptosis, Oncogene 19 (51) (2000) 5851–5857.
[29] M. Ivan, et al., HIFalpha targeted for VHL-mediated destruction by proline hydroxylation: implications for O2 sensing, Science 292 (5516) (2001) 464–468.
[30] B. Lu, et al., Identification of NUB1 as a suppressor of mutant Huntington toxicity via enhanced protein clearance, Nat. Neurosci. 16 (5) (2013) 562–570.
[31] Y. Yao, B. Lu, NUB1 suppression of huntington toxicity: mechanistic insights. Research and Reports in Biochemistry, Res. Rep. Biochem. 5 (5) (2015) 129–136.